STAR Note SN0441

"Resolution" in particle identification with TPCs.

Hans Bichsel

Telephone: 206-329-2792, FAX: 206-685-4634
e-mail: bichsel@sleepy.npl.washington.edu
Center for Experimental Nuclear Physics and Astrophysics
Box 354290 University of Washington
Seattle, WA 98195-4290

reso441.tex 18.11.2002

Abstract.

Theoretical calculations of ionization spectra in a TPC will give better approximations to measurements than the Gaussian functions used currently. Discrimination for dE/dx particle identification (PID), can be improved by taking into account the length of particle tracks. In order to understand that, a distinction must be made between "dE/dx", the *truncated mean dE/dx along a track*, and the *mean truncated mean dE/dx of many tracks* for a given particle type. Several methods for PID inspired by the simulations are proposed. Examples are given for pions and kaons.

I. Introduction.

PID is based on the fact that particle momentum is given by $pc = Mc^2\beta\gamma$, while ionization is dependent on particle speed $\beta\gamma$ only. Thus we need to measure momentum and ionization of particles with mass M along their tracks. A good introduction to the subject is given in Section 9 of [1], but [2] should be consulted for details.

Calculations relevant to PID have been made and presented over several years [3, 4, 5, 6, 7, 8]. Here examples are given which show the improvement in PID which can be achieved if track length is taken into account explicitly [2, 9].

Good agreement was found between energy loss spectra measured in the STAR TPC and those calculated with the theory of atomic collisions [9]. Therefore we can hope to obtain a more detailed understanding for PID from theoretical simulations of the TPC than what we can get from experimental data. An example of experimental data can be seen in Fig. 27.5, p. 010001-212 of [10]. I shall show that the dependence of "dE/dx" on x should be taken into account.

The calculations presented here are obtained with Monte Carlo simulations [3] for individual particle tracks and the subsequent analysis of the distributions for many tracks. The PID analysis is done with truncated mean values and with likelihood values. The "resolution" in PID is defined by "overlap" numbers. Overlap numbers depend strongly on the total length of the track measured and the number of segments in the track.

II. Concepts.

A. Ionization along tracks

To understand and describe PID clearly, it is preferable to replace the concept "dE/dx" currently in use by the concepts described in Fig. 1. The description of the ionization process used here differs somewhat from that used e.g. in [1]. A track is defined as the trace of ionization left by the passage of a fast charged particle through a TPC. The geometry of the detection apparatus consists of

- the measurement of the drift time interval of the electrons produced by one particle and
- the areas defined by the pads in the TPC.

This defines discrete volumes V_i in which the ionization I_i is measured. The length of track through V_i is called the segment length x_i.

A track consists of n segments with lengths x_i. The total track length is $t = \sum^n x_i$. The energy loss Δ by a particle can be described by the number of collisions and the associated energy loss per collision [3, 11]. In some papers, the concept of clusters is used [1]. For the STAR TPC the detection of clusters is not practical. Therefore the total energy Δ_i deposited in the gas in V_i by the particle is considered as the primary datum. This deposited energy leads to ionization $I_i = \Delta_i/W$, where I is the number of electron-ion pairs produced in the gas, and W is the energy needed to produce one ion pair. The observed quantity is the output of the devices (proportional counters, amplifiers, ADCs) which convert I into the recorded datum J. Here, it is assumed that a calibration factor will be determined which relates J_i to Δ_i [9]. The quantity called "dE/dx" is equal to J/x.

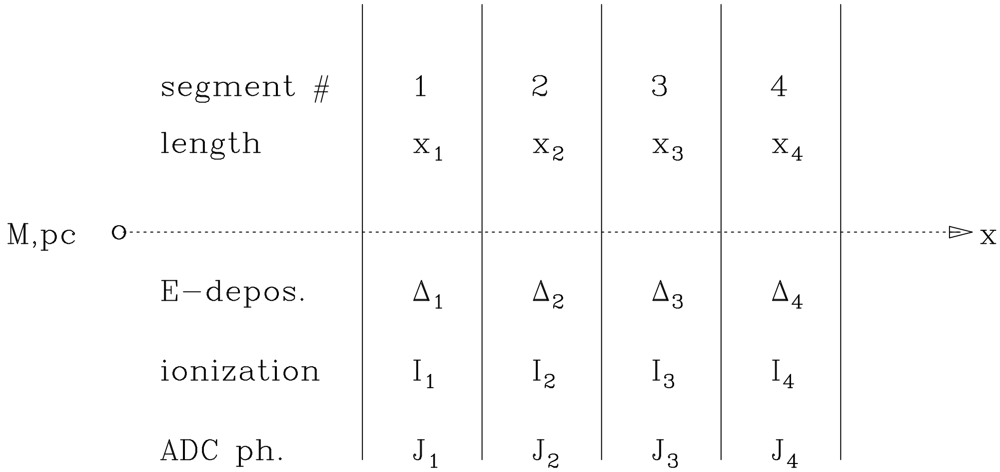

Figure 1: Structure of a particle track.

Track lengths in the STAR TPC vary widely. A track may contain segments from up to 13 inner pad rows with track length $x \geq 1.2$ cm, and from up to 32 outer pad rows where $x \geq 2$ cm. Therefore, a straight track perpendicular to the beam axis can have a length of up to $t = 13 \cdot 1.2 + 32 \cdot 2 = 79.6$ cm. An experimental data set of $1.4 \cdot 10^8$ segments [12] contains values of x up to 4 cm. Thus some tracks could be as long as 160 cm. It will be seen that the overlap numbers show a much stronger dependence on t than do RMS values. It is the purpose of this Note to show that taking into account track length in the PID analysis will improve it.

B. Similarities of straggling functions

Straggling functions for single segments, $f(\Delta; \beta\gamma, x)$, are similar in shape but differ in the location of the most probable energy loss Δ_p and the fwhm w. The similarities are shown in Figs. 2 and 3, where the abscissa is scaled. In Fig. 2, the differences in $f(d)$ for $\Delta > 4$ keV will not cause serious problems for the methods using truncated means.

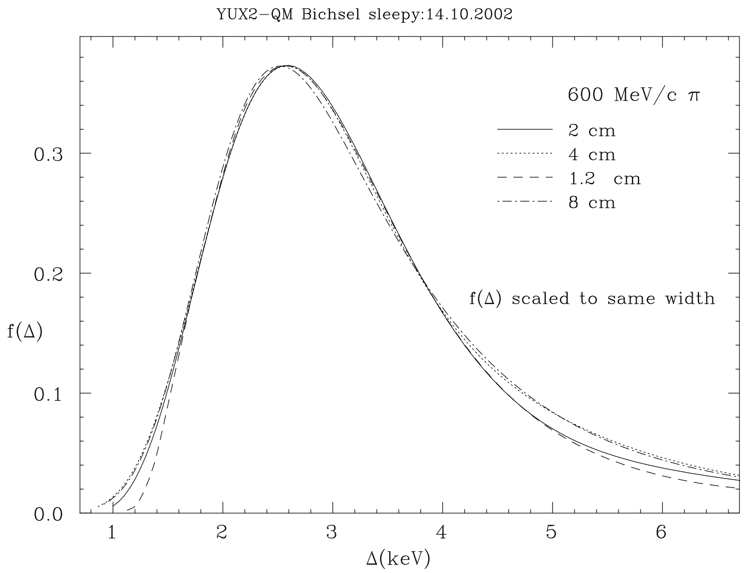

Figure 2: Straggling functions $f(\Delta; x, pc)$ for the same pc and several x. The functions are seen to be similar if linear scaling is used, i.e. $\Delta_x = a + b \cdot \Delta_r$ where r represents a reference function for a certain thickness of gas, and x represents the function for a different thickness of gas. The function for $x = 2$ cm is the reference. The number of Δ above 4 keV is about 30%. Most of these Δ will not be included in the values of the truncated mean for a track.

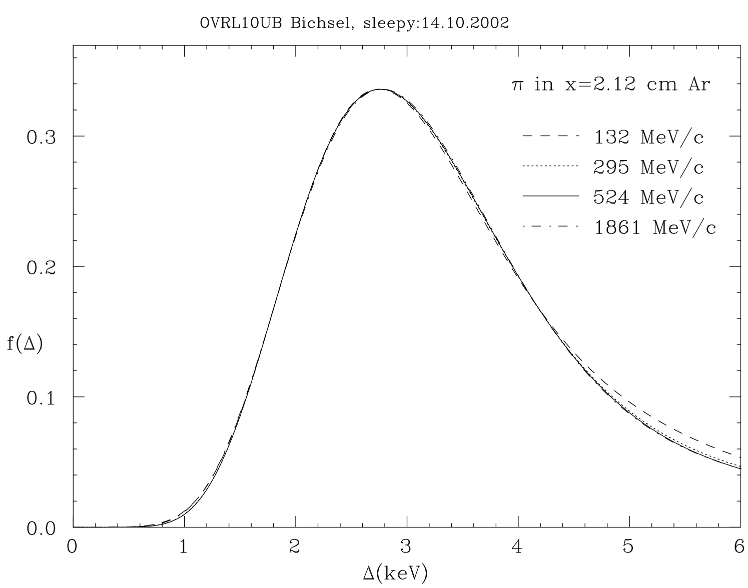

Figure 3: Straggling functions $f(\Delta; x, pc)$ for the same x and several pc. The functions are seen to be similar if linear scaling is used, i.e. ${}_P\Delta = c + d \cdot {}_R\,\Delta$ where R represents a reference function for a certain momentum, and P represents the function for a different momentum, .

C. Truncated mean of energy losses

The *truncated mean value* of the observed single segment values J_i/x of a single track (with index j) with n segments, is defined by

$$d_j = \frac{1}{rn} \sum_{1}^{rn} J_i/x \qquad (1)$$

where r is the truncation factor, between 0.6 and 0.7 for STAR TPC (see Sect. 9.3 in [1]). *I believe that the quantity d also is called dE/dx.* For a large number of tracks of a given track length t and the same number of segments we obtain a distribution function $f(d)$ for which the mean value $< d >$ and the standard (RMS) deviation σ can be calculated. A calculated example of $f(d)$ is shown in Fig. 4 for pions and kaons with momentum p=600 MeV/c traversing 12 inner pad rows ($x = 1.2$ cm) and 20 outer pad rows ($x = 2$ cm) in the STAR TPC, with a truncation ratio $r = 65\%$. Note that the functions are almost symmetric, and therefore $< d >$ will differ little from the most probable value d_p, and fwhm $w \sim 2.36\sigma$. *I believe that the quantity* $< d >$ *also is called dE/dx.* It would be better to distinguish clearly between J/x, d and $< d >$.

D. Likelihood method

For the simulations described here, the ratio method can be used, e.g. Eq. 44, p. 283 in [13]. It is used in the following form for a single track (index j)

$$L_j = \sum_{1}^{n} [\log f_1(J_i; x, p) - \log f_2(J_i; x, p)] \qquad (2)$$

where $\log f(J; x, p)$ are the calculated straggling (Landau) functions for particles 1 and 2 with momentum p for segments of length x. This method can be used for curved tracks where x may change continuously along the track. For a large number of tracks, we obtain distribution functions $g(L)$ similar to those shown in Figs. 4, 5 and 6. This method gives overlap numbers which can be as much as 50% smaller than those obtained with the method of truncated means. It is slightly more complex than the former and I have not used it as much. No further results are given here.

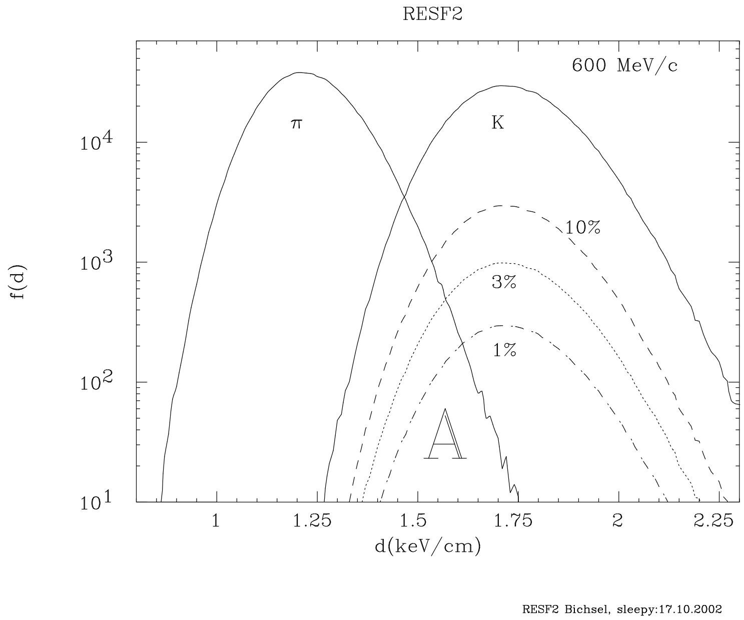

Figure 4: Calculated functions $f(d)$ of truncated mean values d for pions and kaons with momentum $p = 600$ MeV/c traversing 12 inner padrows ($x = 1.2$ cm) and 20 outer padrows ($x = 2$ cm), with $r = 65\%$ truncation. Because of the truncation, the average value of t is 54 cm and includes 21 padrows. The solid lines represent the spectra for 10^6 each of pions and kaons, the broken lines represent reduced fractions of kaons. The **overlap** is defined to be the total number of pions plus the total number of kaons in the area **A**. A **separator** defined by the value d_s at which the lines cross (d_s =1.53 keV/cm for 10%, d_s =1.62 keV/cm for 1%) should be used to derive the number of identified particles. The "separation" of the peaks is given by $s =< d_K > - < d_\pi >= 0.510$ keV/cm and $\sigma_\pi = 0.107$ keV/cm, $\sigma_K = 0.138$ keV/cm.

III. Measures of "resolution".

A. Definitions

In current usage, the "resolution" for PID is defined in terms of the separation s of the two peaks seen in Fig. 4, and a multiple of σ. This means that $f(d)$ are approximated with Gaussians. A more explicit approach is to consider the number of particles given by the area **A** in Fig. 4.

This area is called the "overlap" and gives the number L of particles for which the mass assignment is ambiguous. Here, it is the number of pions plus the number of kaons in **A**. A "separator" defined by the value d_s at which the lines cross is used to derive these numbers. As expected, the separator depends on the fraction of kaons. The spectrum which would be obtained from measurements is given by the solid line in Fig. 5. For $p = 700$ MeV/c, see Fig. 7.

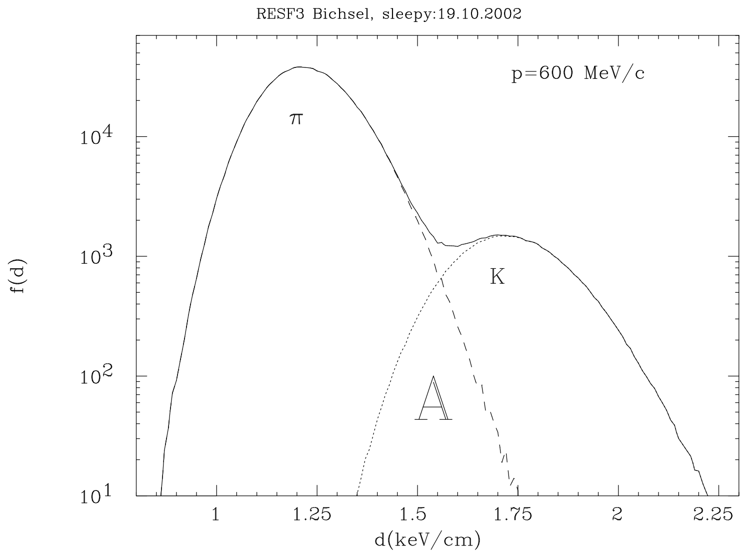

Figure 5: Similar to Fig. 4. The dashed line represents 10^6 pions, the dotted line 50,000 kaons. The solid line corresponds to a spectrum measured in the TPC. The separator is $d_s = 1.56$ keV/cm, and $L = 7370$. The overlap L is approximately inversely proportional to the square root of the ratio of kaons to pions.

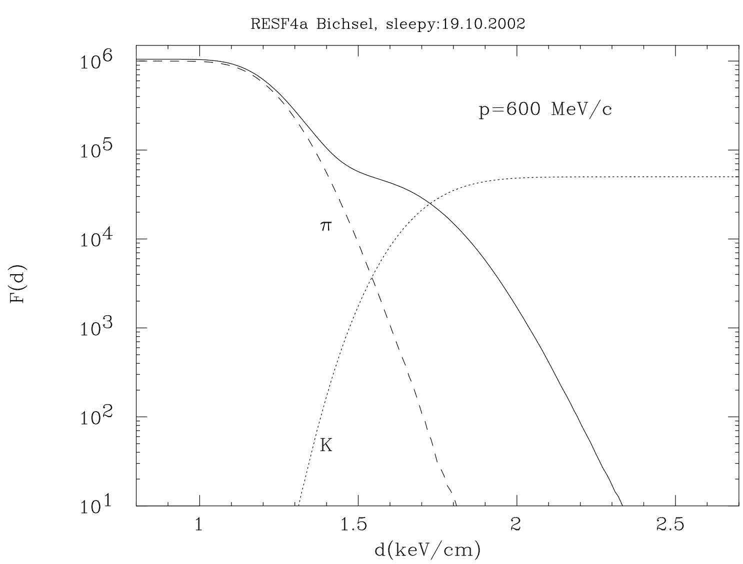

Figure 6: Same as Fig. 5, but using $F(d)$. The solid line corresponds to an experimental observation of $F'(d) = -\int_{\infty}^{d} f(d)dd$. The broken lines are for the separate particles. The cross over point is $d_c = 1.54$ keV/cm. The number $F(d_c)$ for the solid line is the number of kaons in the spectrum.

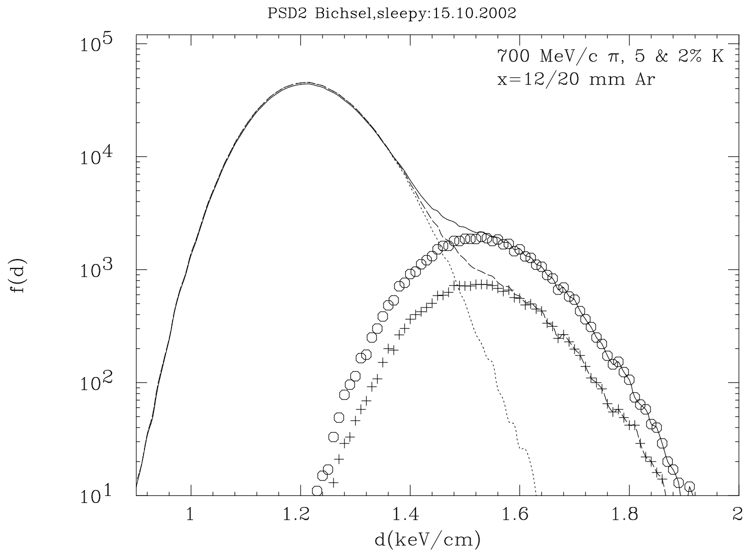

Figure 7: Similar to Fig. 4, for $p = 700$ MeV/c particles.The solid line represents a measured spectrum for 10^6 pions and 50,000 kaons, the dashed line for 20,000 kaons. The dotted line is the calculated function for pions, the symbols represent 50,000 and 20,000 kaons.

An alternative approach can be made by using the integral distribution functions $F(d)$

$$F(d) = \int_0^d f(d)dd \tag{3}$$

In Fig. 6 $(1 - F(d))$ is given for the pions, and $F(d)$ for kaons. Then, equal numbers of particles are in the region of the overlap and their number is given by the value of $F(d_c)$ at the cross over point d_c. Because the functions $f(d)$ are not symmetric, Gaussian fits to them may under-estimate the number of pions in the overlap region by 50% or more. The procedure for the likelihood method is the same.

B. Examples

An example of the influence of the segment length x on the overlap, the value of the truncated means $< d >$ and σ is given in Table I. The calculations are made for pions and kaons with $p = 650$ MeV/c, for $n = 25$ segments with $r = 0.70$ for the six values of x given in the Table. Other examples are given in Figs. 8-11.

Table I. Average values $< d >$ (keV/cm) and $\sigma / < d >$ (%), the cross-over values d_c and overlap fraction L for 50,000 pions and 50,000 kaons for different segment lengths x. In the last line, data are given for a spectrum combined for all the spectra above it.

	π		K			
x(cm)	$< d >$	$\sigma / < d >$	$< d >$	$\sigma / < d >$	d_c	L(%)
2.0	1.328	9.09	1.757	8.64	1.53	5.4
2.2	1.347	8.8	1.781	8.39	1.55	4.9
2.4	1.364	8.54	1.803	8.18	1.57	4.4
2.6	1.380	8.32	1.823	7.99	1.59	4.1
2.8	1.394	8.13	1.841	7.82	1.60	3.7
3.0	1.407	7.95	1.858	7.67	1.62	3.5
$2 \rightarrow 3$	1.37	8.65	1.81	8.29	1.57	4.8

It is seen that $\sigma / < d >$ decreases by about 13%, while the overlap decreases by about 50% with increasing x. Overall, a smaller overlap can be achieved if track lengths cover only a small interval. Note in Fig. 8 that $< d >$ and σ depend not only on track length t, but also on the number of segments. Figs. 9-11 show the strong dependence of the overlap on track length.

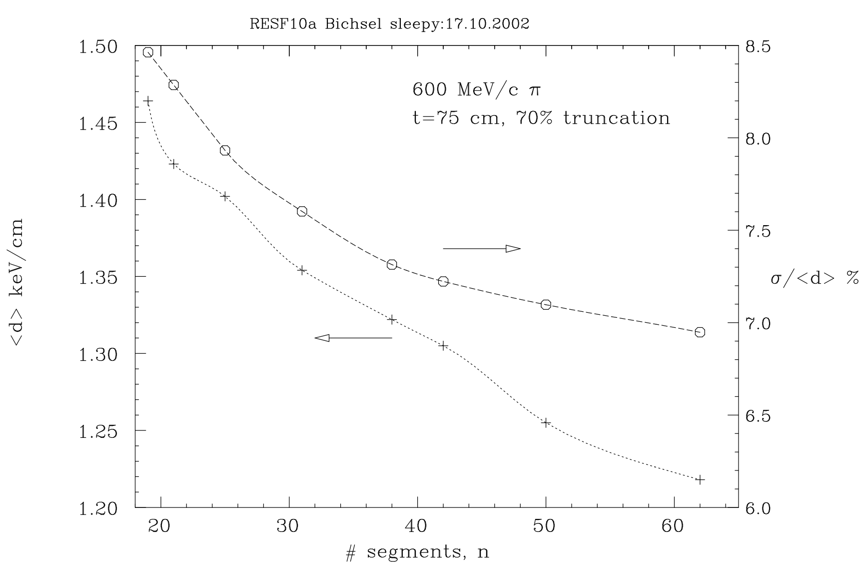

Figure 8: Dependence of $< d >$ and $\sigma / < d >$ on number n of segments for tracks with $t = 75$ cm and $x = t/n$. The irregularities are due to slight variations in t.

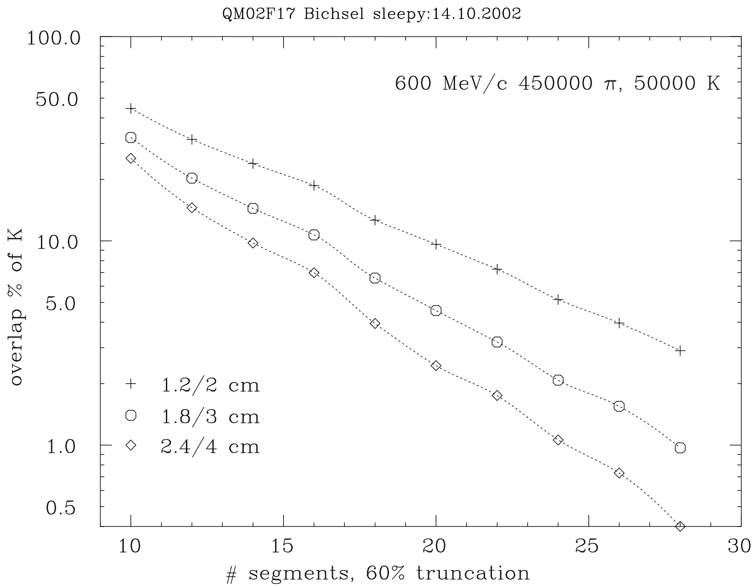

Figure 9: Overlap as a function of track length, which is represented by the number of segments. All tracks include 13 inner segments and an increasing number of outer segments. Thus the number 10 on the abscissa corresponds to 4 outer segments and $t = 24$ cm, the number 26 includes 30 outer segments and gives $t = 75$ cm for $+$, 112 cm for o and 150 cm for $\diamond$.

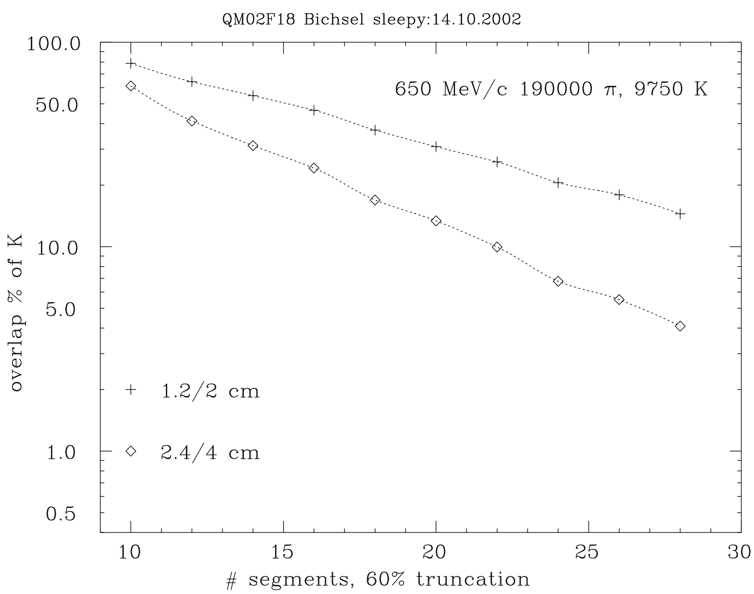

Figure 10: Same as Fig. 9 for $p = 650$ MeV/c.

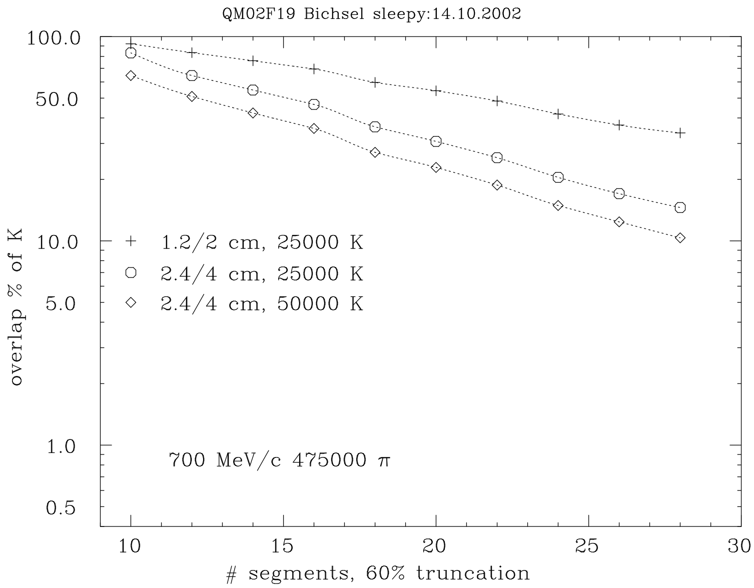

Figure 11: Same as Fig. 9 for $p = 700$ MeV/c.

IV. Practical implementation

.

Computer programs and theoretical functions

During the last few years I have developed many FORTRAN programs which produce the simulations presented here. Some of them are described next.

• ALCOV the primary collision spectrum and the convolutions leading to straggling functions $f(\Delta; x, p)$ for given x and momentum p.

• JCON converts $f(\Delta; x, p)$ to linear scale in Δ and convolutes with the resolution function needed to account for multiplication statistics etc. Examples are shown in Figs. 2 and 3.

• AYYB Monte Carlo simulation of tracks for arbitrary combinations of number of track segments with different x and analysis with the method of truncated means for single particles. Examples are the functions shown in Figs. 4-6.

• BUXU Same as AYYB for two particles. An example are the functions shown in Fig. 7. The cross-over and the overlap values are also calculated, results are shown in Fig. 9-11.

• LKHOOD Same as AYYB, but with the likelihood calculation.

Cross over points and overlap numbers are either obtained directly from BUXU or from graphs like Figs. 4-7 or from the comparison of Tables resulting from AYYB.

I expect that the functions $f(d; p, t)$, Figs. 4,5, and $g(L; p, t)$ will be similar for various p and t

and therefore can be scaled to a few "reference functions" with the method shown for Figs. 2 and 3. So far I have not done that.

Specifically, the program AYYB calculates the functions $f(d; m, r, n_i, x_i, n_o, x_o, p)$ with the truncated mean method, where m is an index for the particle type, r is the truncation ratio, x_i and n_i are segment length and number of inner pad rows, x_o and n_o for outer pad rows and p the momentum of the particle. The moments $< d >$ and σ, as well as the integral $F(d)$ of $f(d)$ are also obtained. Results are shown in Table I.

The program LKHOOD calculates $g(L; m, n_i, x_i, n_o, x_o, p)$ with the likelihood method.

Evaluation of experimental data

Upon examination of Figs. 4-7 it is seen that several methods can be used to determine the type and number of particles found in a measured distribution. If the calibration of J has been made in terms of absolute values of energy deposition Δ (e.g. in keV) as defined in Fig. 1, a measured spectrum $f(d)$ of truncated values will have the appearance of the solid line in Figs. 5, 7 or $F(d)$ of Fig. 6.

- A first estimate of the relative number of pions and kaons in Fig. 4, 5 or 7 can be made by measuring the width of the experimental function at say $f(d) = 100$. Clearly this depends on the fraction of kaons as can be seen in Fig. 4.
- A second estimate can be obtained from Figs. 5 and 6. In Fig. 5 the location d_m of the minimum between the two peaks is determined, then the corresponding number of K at d_m is found in Fig. 6.
- A third estimate can be obtained by comparing the values of $f(d_{p\pi})$ and $f(d_{pK})$ of the two peaks in Fig. 4, where d_p is the location of a peak. Calculated tables for different fractions of particles would have to be made. Once the fraction of particles in a given spectrum has been found, the probability of the mass assignment for a given track can be made from Fig. 6, calculated for the fraction of kaons.
- A fourth estimate can be made with a maximum likelihood search for the number of particles in Fig. 5.

Equivalent estimates can be obtained from the likelihood method, but Eq. (2) requires calculated spectra $f_i(\Delta, x, p)$ for at least two particles. For experimental data the conversion or calibration factor relating J and Δ must be determined [9].

From Figs. 4-7, separators d_s can be chosen which define what fraction of each particle is to be included in the spectrum for the other one. In Fig. 6, for example, the choice of a separator d_s at 1.8 keV/cm would contribute only 1 in 10^5 pions to the kaon spectrum, but it would exclude 70% of the kaons. At the cross-over point d_c in Fig. 6, $d_s = 1.53$ keV/cm, 3500 pions would be included in the kaon spectrum, and 3500 kaons would be included in the pion spectrum.

V. Conclusions

.

We have seen that a better discrimination between different particles can be achieved if the track length t is taken into account. From Table I it is seen that the overlap L is inversely proportional to segment length. Thus a cautious choice might be a spread of $\pm 5\%$ in x. Similarly, it follows from Fig. 8 that the overlap even for a given track length does depend on the segmentation of the track. The strong dependence of overlap on track length t seen in Figs. 9-11 indicates the need for taking t into account in the analysis of experimental data. The function $F(d)$ suggested in Fig. 6 permits the assignment of a probability of mass for a given d. Only a small fraction of experimental data from the full parameter space of the STAR has been compared with theory so far. Thus, further work needs to be done to explore agreement between theory and experiment. For the ultimate in resolution, the likelihood method should be used.

Appendix: low statistics example

.

The calculations in this Note have been made for very large numbers of particles. In practice, this may not be achievable, e.g., for single collisions between two gold nuclei. Evidently it will be necessary to calculate tables of separators and overlap values as a function of several ratios of kaons to pions, see Fig. 4. Also it may be useful to establish tables of the full width at levels of the order of 1%, see Fig. 7.

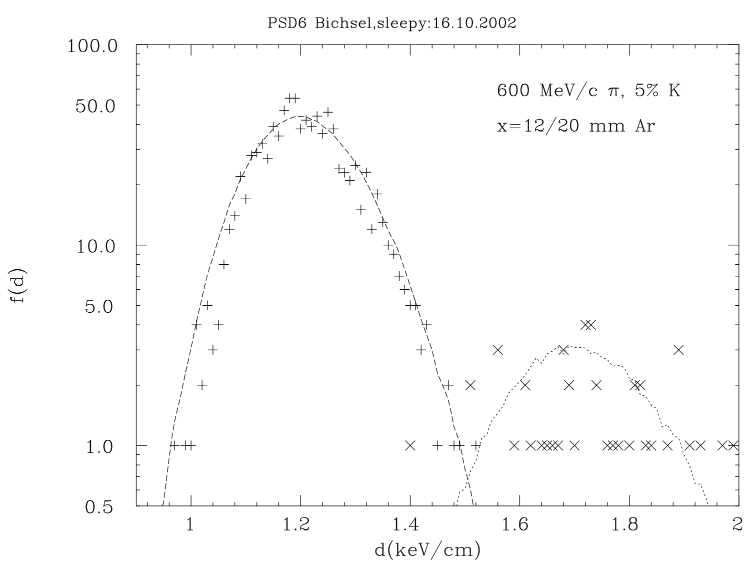

Figure 12: Simulated spectrum for 952 pions and 48 kaons with momentum $p = 600$ MeV/c for $t = 80$ cm and 45 segments. Calculated spectra for 475,000 pions and 25,000 kaons are shown by the broken lines. Clearly, it will be difficult to establish separators from the experimental data, but a calculated separator will give the number of kaons.

Acknowledgments.

I am grateful to my wife Sue who quietly tolerates my neglect of household duties.

References

[1] *Particle Detection with Drift Chambers* W. Blum and L. Rolandi, Springer Verlag, Berlin Heidelberg (1993).

[2] *Comparison of Bethe-Bloch and Bichsel functions.* Hans Bichsel, STAR Note **SN 0439** (3.3.2002).

[3] *Inelastic electronic collision cross sections for Monte Carlo calculations.* Hans Bichsel, Nucl. Inst. Meth. B **52**, 136 (1990)

[4] *Energy loss spectra for argon gas,* H. Bichsel, p. 56, Annual Report, Nuclear Physics Laboratory, April 1993

[5] *Calculation of energy deposition in argon gas for NA35 and NA49 TPCs,* H. Bichsel, p. 57, Annual Report, Nuclear Physics Laboratory, April 1993

[6] *Energy deposition and particle identification in a TPC,* H. Bichsel, p. 46, Annual Report, Nuclear Physics Laboratory, April 1995

[7] *Charged particle-matter interactions.* Hans Bichsel, ch. 87 in Atomic, molecular and optical physics handbook, G. Drake, ed., Amer. Inst. Phys. (1996)

[8] *Energy deposition by low energy electrons in Ar and other gases,* H. Bichsel, p. 49, Annual Report, Nuclear Physics Laboratory, April 1996

[9] *Calculated and experimental Landau spectra in a TPC.* Hans Bichsel, STAR Note **SN 0440** (24.6.2002).

[10] *Review of Particle Physics,* Phys. Rev. D **66** (1 July 2002)

[11] *Straggling in thin silicon detectors.* Hans Bichsel, Rev. Mod. Phys. **60** (1988) 663.

[12] *Private communications* Y. Fisyak, Winter/Spring 2002.

[13] *Relativistic charged particle identification by energy loss* W. W. M. Allison and J. H. Cobb, Ann. Rev. Nucl. Part. Sci. **30** (1980) 253.